Journal of Engineering and Architecture
December 2015, Vol. 3, No. 2, pp. 9-24
ISSN: 2334-2986 (Print), 2334-2994 (Online)

Published by American Research Institute for Policy Development
DOI: 10.15640/jea.v3n2a2
URL: http://dx.doi.org/10.15640/jea.v3n2a2

Mitigation of Air-Blast Pressure Impulses on Building Envelopes through Blast Resistant Ductile Connectors

Daniel Lavarnway[1] & Michael Pollino[2]

Abstract

The rise of intentional or unintentional explosions on both defense critical and conventional buildings requires development of enhanced solutions for the blast protection of structures. This study investigates use of a simple, effective building envelope connector that provides an energy absorbing mechanism for mitigating the effects of a blast event onto a building. The application of the blast resistant ductile connector was assessed by applying principles of conservation of energy and momentum on a generalized single degree of freedom dynamics model (simplified approach) followed by transient nonlinear finite element model to verify the results. The simplified approach allows for rapid design for a range of blast scenarios and potentially varying envelope systems. Conceptual BRDC designs were then evaluated through nonlinear finite element analysis and experimental testing. This study found that the proposed blast resistant ductile connectors were able to safely dissipate the energy for a reasonably wide range of blast scenarios and prevent damage to a minimally reinforced envelope panel.

Keywords: Blast mitigation, Building envelope, Dynamic analyses, Plastic design

1. Introduction

Interest in blast mitigation has increased in the past decade due to the rise in domestic and international terrorist threats. Current design practices utilize mass, ductility, and standoff distance (a secure perimeter) to mitigate the effects of an explosion. These blast mitigation techniques are not always possible to achieve due to location or design constraints. This study explores the feasibility of simple, effective blast resistant ductile connectors (BRDC) implemented between the building envelope and lateral force resisting system(LFRS) which can potentially provide the energy dissipation to absorb the blast or impact while providing a force-limiting mechanism between the building envelope and framing (as illustrated in Fig. 1).

Similar to current blast resistant design procedures (DOD 2008) a balanced design approach must still be employed, however, the ductility and damage would be concentrated into the BRDC for a certain level of blast or impact. Implementation of BRDC could be highly effective and advantageous for blast retrofitting of existing structures since work is concentrated at the exterior and may only require replacement of reasonably accessible connections. Also, repair of newly designed or retrofitted buildings with BRDC will reduce repair downtime following an event since damage is concentrated at the building envelope and not distributed throughout the structural framing that is difficult to access and repair. For high levels of blast and impact, the inherent strength and ductility of the LFRS and envelope may need to be utilized (allow damage) for survival and optimal BRDC behavior might include a secondary hardening phase to engage ductility of the LFRS and building envelope (however this behavior is not considered here).

[1]Designer, Degenkolb Engineers, 600 University St., Suite 720, Seattle, WA 98101. e-mail: dlavarnway@degenkolb.com
[2]Assistant Professor, Dept. of Civil Engineering, Case Western Reserve University, 10900 Euclid Ave, Bingham Bldg. Room 208, Cleveland, OH 44106. E-mail: mcp70@case.edu, Ph. 1-216-368-2778 (Corresponding Author)

This paper presents results of a research study evaluating such blast resistant ductile connectors (BRDC) for blast retrofit and new design of buildings. The research methods use an idealized dynamic/mechanical model for predicting peak BRDC and building panel response which is then verified using nonlinear transient analyses of a building envelope and BRDC. Next, BRDC designs consisting of basic structural shapes which are capable of achieving the desired behavior and do not significantly alter current envelope connection practices, are evaluated through plastic analysis, nonlinear finite element analyses, and experimental testing.

2. Background

Structural design details for mitigating the effects of blast pressures and impact on buildings (structural hardening) relies on predictable ductile failure modes of the building envelope to minimize destruction (DOD 2008, Marchand and Alfawakhiri 2004). Current blast design typically relies on ductility of the building envelope and structural framing and capacity design of the surrounding connections. This is likely based on the assumption that adequate ductility can only be provided in the building envelope and framing. It can be difficult for some types of building envelopes to provide the level of strength and ductility required to resist the dynamic blast pressures without becoming "bunker-like" to provide an adequate level of resistance and difficult in a rehabilitation scenario to upgrade the structural framing to provide adequate ductility and strength. It is also commonly thought that only cast-in-place reinforced concrete structures with their large mass, redundant load paths and ductility can provide adequate blast and impact resistance (Marchand and Alfawakhiri 2004).

Past research has investigated the behavior of structural members and systems under air-blast and projectile impact loading. Naito et. al. (2011) investigated the use of a precast concrete panel system for blast protection of buildings with light gage steel stud walls. The panels could be used for retrofit of existing structures with construction primarily on the structure exterior by connecting the panels with steel angles to the foundation and floor slab. Seica et. al. (2011) developed a finite element-based tool for analysis of architectural glazing subjected to blast loading that is capable of simulating various support conditions. The authors note that support of the glazing panel must be designed to prevent pull-out however inelastic deformation in the framing can provide major benefit for blast resistance. Similarly, Dawson and Smilowitz (2005) recognize the importance of proper balanced design of the building curtain wall system for blast loading and the benefits of allowing large inelastic deformations in the system for protection.

Urgessa and Maji (2010) conducted a series of eight full-scale blast tests on masonry walls with carbon fiber and polymer reinforcement. Resistance is provided primarily through the strength from catenary action of the carbon fiber and polymer reinforcement. Silva and Lu (2009) investigated an analytical procedure for estimating the damage levels in reinforced concrete slabs under various charge weights and standoff distances and verified the procedure utilizing experimental blast testing. Weggel and Zapata (2008) investigated the behavior of laminated glass curtain walls subjected to low-level blast loading. Principal glass stresses were compared for glass with different support conditions representing the silicon and aluminum frame and significant reductions in principal stresses were found for increasing support flexibility (however no material nonlinearity was included in the analysis). Malvar et. al. (2007) investigated the use of composites for strengthening structural components for blast resistance. Naito and Wheaton (2006) developed a methodology for developing the blast resistance of complex load-bearing reinforced concrete shear walls for use in simplified SDOF system blast analysis.

The radial crushing of circular hollow tubes has been studied in past research as an energy absorbing device and is considered in this study for application in blast mitigation of building envelope panels. DeRuntz and Hodge (1963) studied the effects of the radial crushing of a thin, hollow, cylindrical tube and developed a numerical model to predict the load carrying capability of the thin-tube, noting an increase in the load carrying capacity of the section after the initial collapse. Redwood (1964) obtain a more accurate prediction of the load carry capacity of a thin-tube radially crushed between rigid plates by including a bi-linear strain hardening model to the DeRuntz and Hodge equation. Reid and Reddy (1977) further improved the accuracy of the prediction by included an empirical moment arm and a combination of rigid arcs and plastic yielding arcs into the solution which corresponded to the deflection and better represented the experimental results.

3. Prototype Panel and Blast Loading Description

The building envelope panel considered in the investigation is a3.66 by 7.32 by 0.15 meter (height-to-width-to-thickness) pre-cast 34.5 MPa concrete panel. The pre-cast panel is reinforced with only temperature and shrinkage

reinforcement per ACI 318-08 (ACI 2008) and is designed to remain elastic by capacity design to the BRDC and accounting for dynamic amplification (discussed later). The BRDCs are considered to be connected to the exterior building frame on the top and bottom edges of the panel, allowing one-way action in the short direction (as illustrated in Fig. 1). This allows lateral load transfer from the BRDCs directly to the diaphragms and building LFRS and eliminates large forces along the column heights. This however places larger demands on the panel compared to development of two-way action in the panel if connected to the columns. The range of blast protection (charge weights and standoff distances) for this lightly reinforced panel with and without BRDCs is considered in this paper however increasing the panel reinforcement could significantly expand the range of blast protection while keeping the panel elastic.

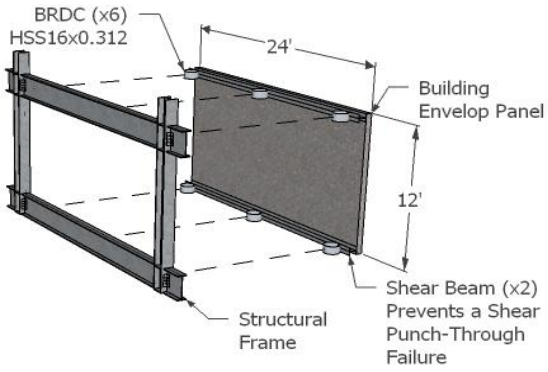

Fig. 1 Implementation of BRDC to Building Envelope Panel

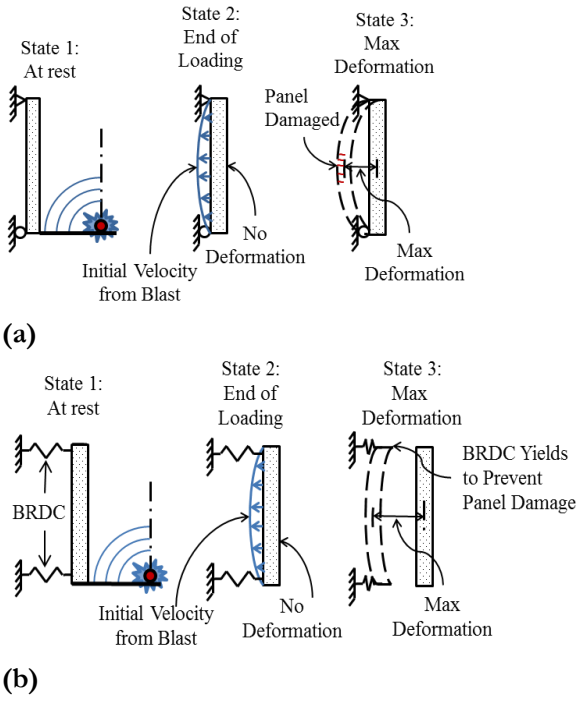

Fig. 2 Illustration of the System Response States (a) without BRDC and (b) with BRDC

The strength and deformation capacity of a 3.66m x 7.32m x 0.15m concrete panel with temperature and shrinkage reinforcement was calculated to determine the limits on the BRDC for protecting a minimally reinforced panel. The yield strength of the panel will provide an upper limit on the strength of the BRDC to provide a balanced design ensuring yield of the BRDC prior to panel yield (damage) and must also have a lower bound required to resist wind pressures. According to the ACI 318-08 (ACI, 2008) the minimum amount of reinforcement per unit length for a 3.66m x 7.32m x 0.15m concrete panel is275mm^2/m. To obtain this amount of reinforcement, #4 bars spaced at 460 mm on-center could be used which would provide 282mm^2/m of reinforcement. The moment that a one-way slab with this amount of reinforcement can resist is equal to 11.9 kN-m/m. The resulting displacement at mid-span of the panel at yield of the temperature and shrinkage reinforcement is equal to 4.1 mm accounting for cracked concrete section properties.

The building envelope and connectors are idealized for theoretical response calculations by an elastic beam, representing a building envelope panel over a typical bay width and story height, and two nonlinear springs, representing the BRDCs, and is illustrated in Fig. 2. The beam represents the panel mass and stiffness considering one-way action of the panel in the short direction. The blast pressures are applied to the system as described in the next section.

3.1. Blast Loading Approximation

The blast pressure time history (P_{rt}) considered in this study is a simplified triangular linearly decaying function representing the positive phase impulse from the blast history shown in Fig. 3. The linearly decaying function begins at time of arrival, t_a. This simplified triangular approximation of the loading is used because it captures the parameters of most interest: the peak reflected pressure (P_r) and the reflected impulse (Im). An adjusted time of duration (t_d) is calculated to give an equivalent impulse of the more complex pressure history. The peak reflected pressure, reflected impulse, and time of duration vary with the charge weight (W) and standoff distance (R). Blast scenarios considered throughout assume a ground explosion located normal to mid-width of the panel. In the interest of actual building security, the loading will be described throughout this paper by the pressure impulse applied to the building envelope and not by the charge weights and standoff distances however the range of impulses considered are those which might commonly be considered for building blast design (FEMA 2005).

Both the peak reflected pressure and reflected impulse (Fig. 3) were estimated using curve-fit equations from Swisdak (1994) of blast tests conducted primarily by Kingery (1966). These equations have been adopted by the Department of Defense Explosives Safety Board and validated by over 30 years of application and supporting test data (Chapman et. al., 2004). The spatial pressure variations across the face of the panel were assumed to be negligible for the blast scenarios considered, assuming a standoff distance greater than 3.66 meter which would make the angle of incidence with the 3.66m x 7.32m panel less than 45 degrees.

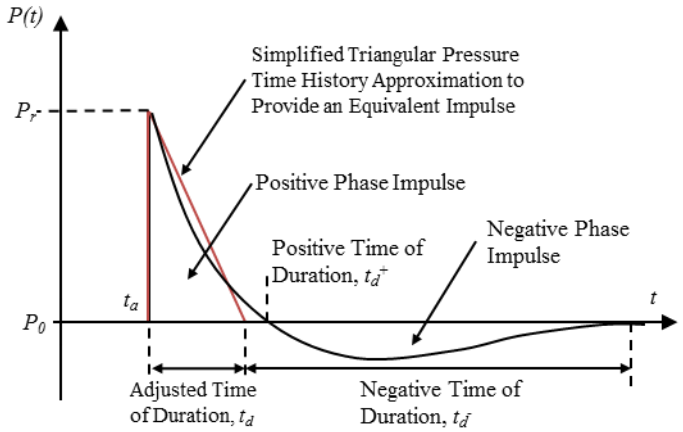

Fig. 3 Free-Field Pressure-Time Variation

It can be shown from methods outlined in Blevins (1993) that the natural period of the reinforced concrete panel is 77.4milliseconds. A load can be considered purely impulsive when the time of duration of the load is less than one-fifth the natural period of the system (Clough and Penzien, 1975).

Comparing the natural period of the concrete panel to the blast loading time of duration, a majority of the blast scenarios can be considered purely impulsive, but there are cases where the loading cannot be considered impulsive, these cases will be explicitly accounted for in the dynamic FEA described later.

The following theoretical calculations will assume a purely impulsive pressure loading and the time variation of the load is not included.

4. Generalized Dynamic-Mechanical Model

To provide an understanding and develop a closed-form derivation of the system response, a simplified single degree of freedom (SDOF) generalized dynamic model (Clough and Penzien, 1975) of the BRDC and wall panel was developed. Neglecting the effects of damping, the generalized equation of motion is:

$$m^* \cdot \ddot{y}^* + k^* \cdot y^* = P^* \tag{1}$$

Where $\ddot{y}^*$ and y* are the generalized out-of-plane acceleration and displacement at the center of the panel, respectively. The assumed deformed shape of the panel, ψ, is the first mode shape of panel which is a half sine wave (Biggs, 1964). Additionally, m* is the generalized lumped mass, k* is the generalized stiffness, and P* is the generalized external pressure defined as:

$$m^* = \int_0^H m \cdot \psi^2 \, dx \tag{2}$$

$$k^* = \int_0^H E \cdot I_{crack} \left(\frac{d^2\psi}{dx^2}\right)^2 \, dx \tag{3}$$

$$P^* = \int_0^H b \cdot P_{rt} \cdot \psi \, dx \tag{4}$$

where m is the mass per unit length along the height of the panel, E is the modulus of elasticity of the precast concrete panel (27.8 GPa), I_{crack} is the cracked moment of inertia of the panel (taken simply as half of the gross moment of inertia), P_{rt} is the simplified reflected blast pressure time history described previously, H is the panel height (3.66m), and b is the width of the panel (7.32 m). The generalized impulse of the blast load is equal to the generalized reflected pressure of the blast acting over the time of duration of the blast:

$$Im^* = \int_{t_a}^{t_a+t_d} P^* \, dt \tag{5}$$

4.1. Peak Response of Panel without BRDC

The peak response of the panel and BRDCs are calculated by applying conservation of momentum and conservation of energy at three different system response states (seen in Fig. 2): 1) the system at rest 2) at the end of the blast loading at 3) at the maximum deformation of the system. From state one to two, purely impulsive loading imparts an instantaneous velocity onto the panel. Since the panel is initially at rest, the velocity at the second state can be determined from conservation of momentum and is equal to:

$$vel_2 = \frac{Im^*}{m^*} \tag{6}$$

Conservation of energy was used to calculate the response from the end of loading (state 2) to the point of maximum deformation and zero velocity (state 3):

$$PE_2 + KE_2 + W_{23} = PE_3 + KE_3 \tag{7}$$

Assuming no BRDC (W_{23} equals zero) and that the panel responds elastically, the kinetic energy at state 2 (KE_2) is equal to the potential energy at state 3 (PE_3):

$$\frac{1}{2}m^*\left(\frac{Im^*}{m^*}\right)^2 = \frac{1}{2}k^* \cdot U^{*2} \tag{8}$$

where U* is the generalized maximum displacement of the mid-span of the concrete panel. Rearranging Eq. (8), the generalized maximum displacement of the panel without BRDCs becomes:

$$U^* = \frac{Im^*}{\sqrt{m^* \cdot k^*}} \tag{9}$$

The displacement at the mid-span of the concrete panel has been plotted against blast scenarios with varying impulses in Fig. 4. Additionally, a horizontal line is seen in the figure which represents the peak deformation limit of the panel with only temperature and shrinkage (T+S) reinforcement. Therefore, the blast scenarios that are above the T+S line would result in a deflection greater than the allowable, causing the panel to yield. As Fig. 4 shows, a majority of the blast scenarios considered would yield or fail with T+S reinforcement alone.

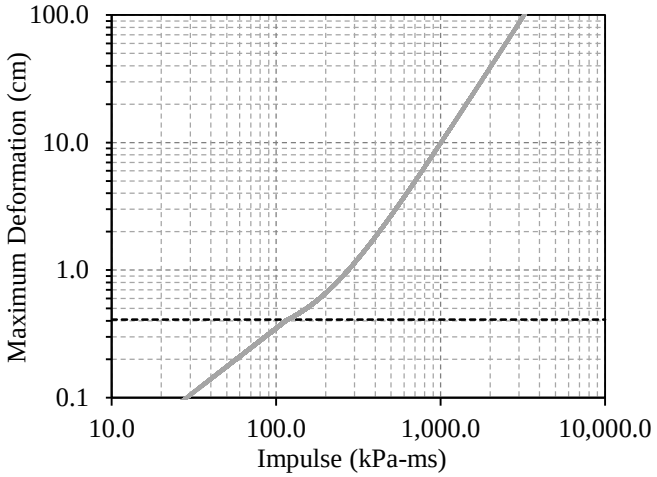

Fig. 4 Maximum Deformation at Mid-span of the Panel (Without BRDC) caused by a Blast Events with Varying Impulses

4.2. Peak Response of Panel/BRDC System

Including the BRDCs has no effect on the initial velocity imparted to the panel since the BRDCs do not change the system mass and assuming essentially rigid BRDCs (compared to the panel), the natural period of the system does not change and the loading can still be considered purely impulsive. Therefore, only the conservation of energy expression changes from the case of no BRDCs and non-conservative external work (W_{23}) is added from the plastic deformations of the BRDC and it is equal to:

$$W_{23} = -2 \cdot F_{ye} \cdot \left(\delta_c - {}^1\!/_2 \cdot \Delta_{ye}\right) \tag{10}$$

where δ_c is deformation of the BRDC, F_{ye} is the yield force of all BRDCs on one edge of the panel, and Δ_{ye} is the BRDC yield displacement. This calculation of work done by the BRDC is based on the assumption of elasto-plastic behavior. Thus, the conservation of energy formula (Eq. (7)) becomes:

$$\frac{1}{2}m^* \cdot vel_2{}^2 - 2 \cdot F_{ye} \cdot \left(\delta_c - {}^1\!/_2 \cdot \Delta_{ye}\right) = \frac{1}{2}k^* \cdot U_{equiv}{}^2 \tag{11}$$

where U_{equiv} is the elastic displacement of the mid-span of the concrete panel at BRDC yield and vel_2 is determined from Eq. (6).

Following the impulse, the BRDCs yield and impart a force in the panel which is conservatively considered to be an impulsive rectangular load (zero rise time). A rectangular impulsive load applies a dynamic amplification factor (DAF) equal to two times the static response of the system for Δt to T ratio of 0.5 or greater (Biggs 1964), where Δt is the time of duration of the rectangular load pulse and T is the natural period of the system. The natural period of the generalized system, T* is equal to 77.4 ms and the time of duration of the rectangular load pulse applied by the BRDC can be determined through the conservation of momentum and is equal to:

$$\Delta t = \frac{Im^*}{2 \cdot F_{ye}} \tag{12}$$

The resulting $\Delta t/T^*$ ratios were calculated for the range of charge weight, standoff distances, and BRDC yield forces and the majority of scenarios have $\Delta t/T^*$ ratios greater than 0.5 and thus, the DAF will be assumed a value of two and this assumption is verified in by the dynamic FEA discussed later. Therefore, from a design standpoint, the maximum yield force of the BRDC to allow for elastic panel behavior is equal to half the equivalent static reactions at the ends of the panel at yield of the panel at mid-span which is equal to 47.6 kN for the panel sizes and reinforcement considered.

Rearranging the terms of (11) into a quadratic formula to solve for the yielding force of a panel edge, F_{ye}:

This equation was solved numerically for the required BRDC edge yield force, F_{ye}, varying values of δ_c from 0 mm to 300 mm and varying the initial panel velocity, vel_2, based on different blast scenarios with impulses ranging from

$$k^* \left[\frac{10 \cdot Len^3}{384 \cdot E \cdot I_{crack}}\right]^2 {F_{ye}}^2 + 4 \cdot F_{ye} \cdot \left(\delta_c - {}^1\!/_2 \cdot \Delta_{ye}\right) - m^* \cdot {vel_2}^2 = 0 \tag{13}$$

100 to 800 kPa-ms. To ensure the panel was protected and remained elastic, F_{ye} was set to forces below 47.6 kN (the allowable force for the panel considered) and a lower bound value of 13.3 kN was used based on the required BRDC capacity to resist wind pressure on the panel per ASCE 7-10 (ASCE 2010). So, the BRDC will yield and deform before the panel yields. A zero millimeter deformation of δ_c represents the case without BRDCs (zero non-conservative work taken from the system). The results of the calculations representing acceptable BRDC force and deformation design demands, panel remained elastic, are plotted for varying impulses in Fig. 5. Recall that a 3.66m x 7.2m x 0.15m concrete panel with temperature and shrinkage reinforcement alone can only deform a total of 4.1 mm. Without the BRDCs this panel would only be able to withstand a blast impulse of approximately 120 kPa-ms, as shown by Fig. 4 at the intersection of the temperature and shrinkage limit curve. If the BRDC is able to deform approximately 12.0cm, it increases the blast resistance of the panel with only temperature and shrinkage reinforcement significantly, being able to withstand a blast impulse of greater than 700 kPa-ms as seen in Fig. 5. Allowing for larger BRDC yield forces (through panel strengthening) and deformations (by larger designed panel offsets) can further increase the blast resistance of the building envelope while possibly preventing damage to the envelope itself.

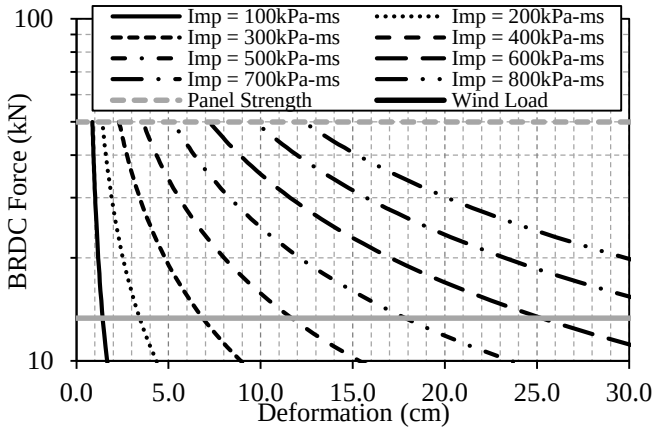

Fig. 5 BRDC Deformation given a BRDC Yield Force for Various Blast Impulses

5. Nonlinear Dynamic Finite Element Analysis of BRDC-Panel

5.1. Model Description

A nonlinear transient finite element model was created to verify the results obtained by the theoretical evaluation. The finite element program ANSYS (Ver. 14) was used for the analysis.

The 3.66m x 7.2m x 0.15m concrete panel was considered to be connected at the top and bottom by six BRDCs, three along the top and bottom edges each as shown in Fig. 1, based on standard façade panel connection practices. The panel was modeled using 4-noded thick shell elements (ANSYS shell181) with an element size of 63 mm based on a convergence study.

The BRDCs were modeled using truss elements (ANSYS link180) to produce an elasto-plastic force-deformation behavior. An axial truss element was used for modeling simplicity to develop a general elasto-plastic behavior however actual BRDC designs could yield in flexure, shear, torsion, axial, etc. A plasticity material model with bilinear kinematic hardening was assigned to the elements. For analysis purposes, the area of the truss elements was varied in order to control the BRDC yield force. Note that the BRDC yield force that was developed previously was the sum of the actual BRDC yield forces along an entire panel edge and not the individual BRDC yield force being considered here. The length of the truss elements was calculated to produce a BRDC yield displacement of 1.5 cm based on the observed yield displacement from the proposed BRDC designs presented later. The yield displacement does not however have a significant impact on panel response for cases where the maximum displacement significantly exceeds the yield displacement which would be typical for design level loading scenarios. This analysis assumed that the lateral force resisting system (LFRS) would remain rigid throughout the blast event. Thus, all the DOFs of the node at the end of the BRDC that would connect to the LFRS were restricted to zero. To prevent a shear punching failure of the BRDC through the concrete panel some amount of edge strengthening would be required in design.

The blast loading was a uniformly distributed pressure load applied to the face of all shell elements in the out-of-plane direction. The pressure time-history for the finite element analysis (FEA) was the same pressure time-history used in the theoretical analysis, a linearly decaying function with time. The pressure loading was defined at time steps of 0.0005 seconds. This load step is appropriate given the blast loading time of durations considered, the average of which is 0.023 seconds, 46 times greater than the load step. A convergence study was performed to ensure that the model had an adequate mesh resolution to capture the effects of the different modes being excited within the panel.

5.2. Analysis Cases Considered

Analyses were performed for three or more different BRDC yield forces for every blast scenario. The BRDC yield forces targeted a panel edge yield force between 13.3 kN and 46.7 kN for reasons described previously. Blast scenarios were considered that generated 100 – 800 kPa-ms impulse which are within a reasonable range for design based on FEMA (2005).

5.3. Analysis Results

The force in all BRDCs (three on each of the longer edges) and the displacements at a corner, middle of long and short edge, and center of the panel were extracted from each analysis. The maximum force and the corresponding deformation for each BRDC were calculated. The relative displacement between the center and edge of the panel was also calculated to determine if it exceeded the elastic displacement limit of the panel of 4.1 mm. For the blast scenarios analyzed, approximately 50% resulted in a relative displacement greater than 4.1 mm. The relative displacements had a maximum value of 6.61 mm and an average value of 3.60 mm. Results of BRDC deformations from the nonlinear transient finite element model are presented with the results from the theoretical model in Table 1. The deformation results of the nonlinear transient FEA correlated well with the results of the theoretical evaluation with a median difference of 9.1%.

Table 1. Transient Finite Element Analysis Cases and Results

Case#	Impulse (kPa-ms)	BRDC Yield Force (kN)	FEA Results		Theoretical Model	%Diff, BRDC Disp (Theoretical vs. FEA)
			BRDC Disp (cm)	Diff. Panel Def. (mm)	BRDC Disp (cm)	
1	46.0	46.7	0.44	1.26	0.75	-72.5
2	46.0	13.4	0.82	0.70	0.97	-17.8
3	140.0	46.7	1.34	3.86	1.31	2.2
4	140.0	13.4	2.88	1.51	2.91	-1.0
5	436.2	46.7	6.73	6.55	6.75	-0.2
6	436.2	13.4	21.24	1.98	21.94	-3.3
17	154.9	46.7	1.60	4.55	1.45	9.2
18	154.9	37.8	1.81	4.02	1.64	9.3
19	154.9	13.4	3.77	1.56	3.41	9.5
20	249.4	46.7	3.04	5.28	2.67	12.1
21	249.4	42.3	3.27	4.82	2.89	11.7
22	249.4	13.4	8.59	1.77	7.68	10.6
23	470.1	46.7	8.81	6.61	7.75	12.0
24	470.1	44.9	9.13	6.36	8.03	12.1
25	470.1	31.2	12.76	4.58	11.30	11.5
26	470.1	13.4	27.97	1.99	25.44	9.1
27	95.2	46.7	0.98	2.79	0.98	1.0
28	95.2	42.3	1.04	2.71	1.01	2.5
29	95.2	23.4	1.40	2.02	1.29	7.9
30	95.2	13.4	1.90	1.31	1.74	8.5
31	177.6	46.7	1.90	5.09	1.69	10.6
32	177.6	37.8	2.19	4.26	1.94	11.4
33	177.6	23.4	3.07	2.71	2.72	11.6
34	177.6	13.4	4.83	1.57	4.26	11.9
35	284.9	46.7	3.74	5.48	3.28	12.3
36	284.9	44.9	3.85	5.29	3.39	12.0
37	284.9	13.4	11.17	1.79	9.82	12.1
47	200.2	46.7	2.13	5.06	1.97	7.4
48	200.2	37.8	2.50	4.23	2.28	8.7
49	200.2	13.4	5.91	1.59	5.22	11.6
50	321.0	46.7	4.21	5.48	3.99	5.2
51	321.0	42.3	4.60	5.08	4.34	5.6
52	321.0	13.4	13.74	1.68	12.30	10.5
53	514.4	46.7	9.53	5.84	9.18	3.6
54	514.4	44.9	9.90	5.63	9.52	3.8
55	514.4	33.4	13.46	4.34	12.60	6.4
56	514.4	13.4	33.24	1.78	30.45	8.4

6. Proposed BRDC Design

A number of potential BRDC designs have been considered (Lavarnway 2013) however the behavior and test results of round hollow structural sections (HSS) are described here. A round HSS is a standard structural steel shape and therefore is believed to be a cost-effective, economical design. It also offers a wide range of parameters for BRDC design such as the length, radius, and thickness. The round HSS would be expected to dissipate blast energy by plastically deforming radially inward forming four yield lines. Only the blast loading transferred to the BRDC is considered in this study.

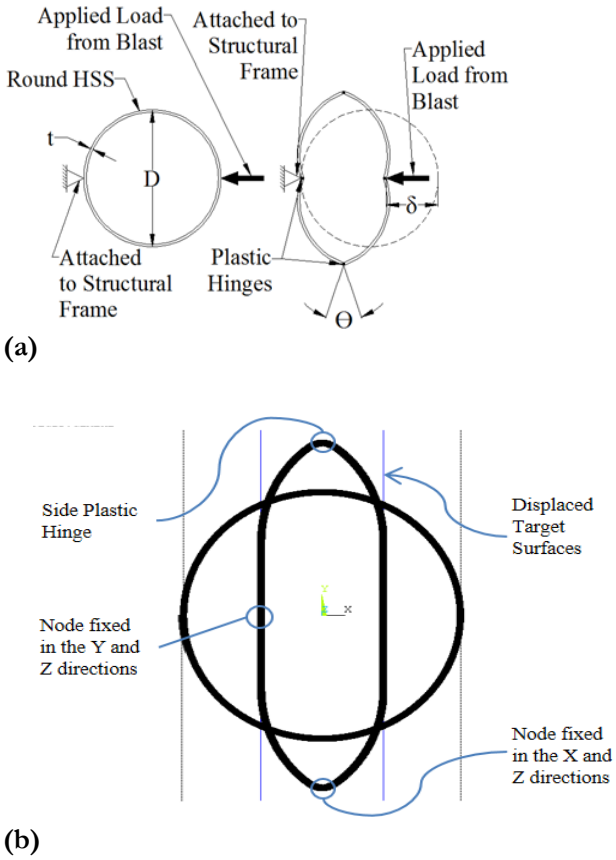

Fig. 6 Potential Loading and Support Conditions for Round HSS
(a) Point Load/Support and (b) Contact Surfaces

It is anticipated that the round HSS could be connected between the panel and exterior framing in a configuration that either applies a concentrated line loads or effectively provides a contact surface at two sides of the HSS as illustrated in Fig. 6. A typical facade connection detail (Parker, 2008) with a round HSS (contact surface) BRDC inserted between the stiffeners of the spandrel beam are shown in Fig.7. This connection detail is shown for illustrative purposes only and may differ in practice, depending on the structural framing and building envelop detailing.

The resulting plastic compressive capacity (P_p) of a round HSS subjected to a concentrated line load and reaction along its length can be determined using concepts of plastic analysis and shown to equal:

Where is the unreformed radius of the round HSS, f_y is the expected material yield stress, t_w is the HSS wall thickness, and b_B is length of the section. A sample set of design curves for this loading/support condition relating the HSS length to the wall thickness have been plotted in Fig. 8 to achieve the maximum force per connector of 15.6 kN per BRDC assuming a material yield stress of 290 MPa (A500 Gr. B). The required BRDC sizes fall within many of the

$$P_p = \frac{b_B \cdot {t_w}^2 \cdot \mathrm{f_y}}{\mathrm{r}} \tag{14}$$

commonly available round HSS shapes (AISC 2005). DOD (2008) recommends design plastic hinge rotation capacities of 12 degrees for flat steel plates in bending however, as will be shown in further analysis and experimental testing, a much larger plastic rotational capacity can be achieved with the round HSS. The contact support condition produces a more complex behavior as the HSS deforms and additional support and loading points develop and is considered in the following analysis and experimental testing.

However, Eq. (14) still provides a reasonable prediction of the initial plastic capacity that could be used for design. The round HSS sections were found through plastic analysis to develop the necessary yield forces to satisfy blast

design objectives over a wide range of blast loading scenarios. Therefore, the HSS sections were investigated further through nonlinear FEA and quasi-static experimentation.

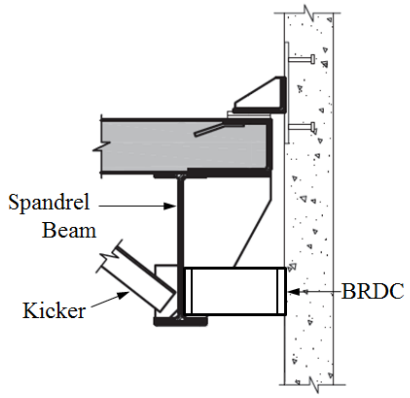

Fig. 7 Potential BRDC Implementation Details

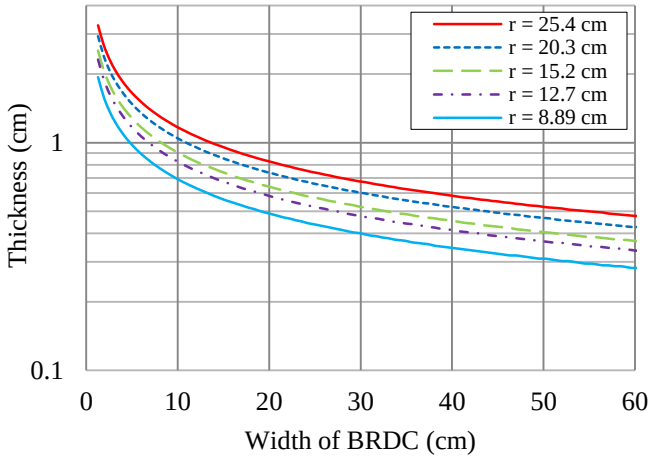

Fig. 8 Round HSS BRDC Design Curves for a Target Strength of 15.6 kN

6.1. Nonlinear Static Finite Element Analysis of Round HSS BRDCs

The force-deformation behavior and stress-strain response of the proposed round HSS BRDCs were further investigated through use of static analysis of the round HSS. The analyses include both material and geometric nonlinearity. While both support and loading conditions have been evaluated (Lavarnway 2013), the results of the contact surface analyses are presented here. Three round HSS sections (HSS16x0.375, HSS10.75x0.25, and HSS7x0.25) were selected to be evaluated with a boundary plane support/loading condition (Fig. 6) and were also tested experimentally (discussed later).

6.1.1. Model Description

The round HSS BRDC was modeled in ANSYS using Timoshenko beam elements with nonlinear material behavior (ANSYS beam189). These beam elements were modeled as a two dimensional unit width model with a rectangular cross-section which assumed a uniform support and loading condition along the tube length. A convergence study performed on the total Von Mises strain to ensure accuracy of the solution.

A total of 2000 beam elements around the circumference and 18 cells through the thickness and width of the cross-section were found to be adequate. A coarser element size could have been utilized outside of the plastic hinging regions.

Table 2 BRDC Experimental Specimen Details

Section	Grade of Steel	Measured yield stress (MPa)	Measured Tensile Stress (MPa)	Measured Thickness (mm)	Section Length Tested (mm)	Exp. Yield Force (kN)	Yield Force Eq. (14) (kN)
HSS16x0.375	A53 Gr. B	380	516	9.78	203	37	36.3
HSS10.75x0.25	A106 Gr. B	406	477	6.48	203	25	25.3
HSS7x0.25	A513 Type 5	772	848	6.40	140	44	49.8

Due to local availability and cost of the experimental specimens, sections with different material grades were tested as noted in Table 2. A multi-linear isotropic hardening model was utilized and adopted a tri-linear isotropic hardening model described by Okazaki (2004). This model was developed for grade A992 steel and was modified to represent the expected yield

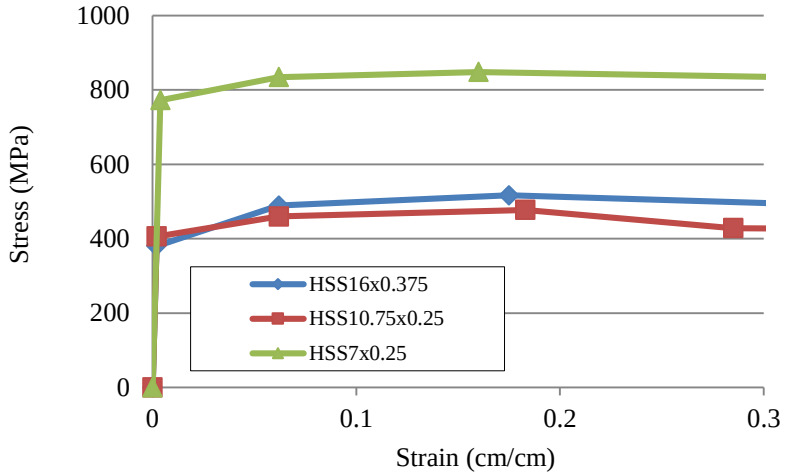

Fig. 9 Stress-strain Values used in the Multi-linear Hardening Material Model

Stress and ultimate tensile stress of the materials tested and the large strains expected to be developed. Stress-strain values for the multi-linear isotropic and hardening model used are displayed in Fig. 9.

This analysis requires the use of contact elements and target surfaces to simulate HSS contact with the boundary plane (ANSYS conta172 and targe169, respectively). The boundary planes were modeled as the target surface while the contact elements were used to model the contact surface around the beam189 elements (the round HSS BRDC). The model was loaded by enforcing a 76 mm inward displacement of the boundary planes while preventing lateral movement of the HSS at contact points as illustrated in Fig. 6.

6.1.2. Results

The force-deformation results of the nonlinear FEA of the boundary plane support/loading condition are shown in Fig. 10 to 12 and critical response values also provided in Table 3.

Table 3: BRDC FEA Results

Section	Stress at Side Hinge (MPa)	Strain at Side Hinge (%)	Yield Force (kN)
HSS16x0.375	484	5.94	34
HSS10.75x0.25	476	27.5	25
HSS7x0.25	853	26.3	45

As expected and noted in Table 3, the stress and strain increases as the diameter decreases, because each section is exposed to the same 152 mm displacement thus the smaller diameter sections must go through larger rotations. The

stress and strain values for the HSS7 are very high due to the large rotations at the side plastic hinges which were estimated by simplified rigid plastic kinematic hand calculations to be 57° at a 152 mm deformation.

The yield force observed in the force-deformation curves compare well with the calculated plastic capacity of the sections from Eq. (14). Beyond yield there is a region of reasonably constant plastic deformation followed by material and geometric hardening during radial crushing of the round HSS which has been documented by Reid and Reddy (1977). The boundary support plane results in increased load carrying capacity at large deformations as seen in Fig. 10 and Fig. 12. As a round tube is crushed between two rigid plates the contact width increases and the moment arm between plastic hinging regions deceases which requires an increased load to achieve the same deformation. The deformed configurations are highlighted in the photos in the figures. The significant increase in load carrying capacity of the smaller HSS is due to the geometrical hardening effects being more severe for smaller diameter tubes.

6.2. Quasi-Static BRDC Experiments

A series of HSS members were tested for verification with the analytical results and to evaluate the ultimate failure condition of the members under radial loading. All experiments were carried out on a 1000 kN capacity MTS servo-hydraulic compression test system. The hydraulic actuator includes an in-line load cell and LVDT to measure the displacement and force applied. The MTS system has a maximum stroke of 127 mm. Thus, all compression tests were done in 120 mm displacement segments, resetting the crosshead and reloading after each segment. The re-setting of the cross-head did elastically unload and re-load the specimen; however, this has no impact on the force-deformation results and the unloading and re-loading data was removed from the experimental results for clarity.

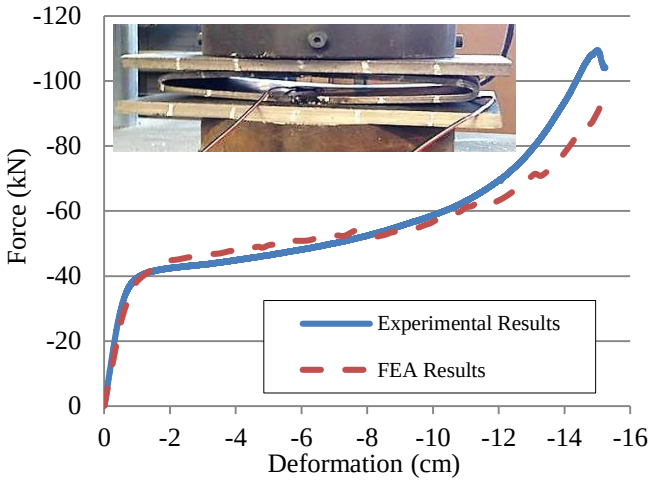

Fig. 10 Force-Deformation Response of a Round HSS7x0.25 and Deformed Configuration at Approximately 152 mm

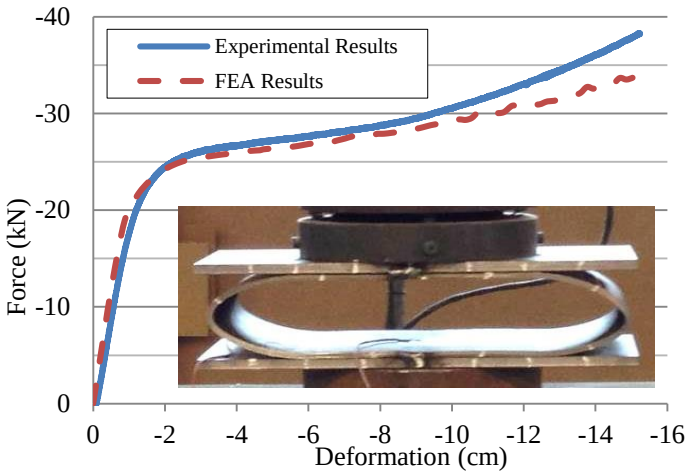

Fig. 11 Force-Deformation Response of a Round HSS10.75x0.25 and Deformed Configuration at Approximately 152 mm

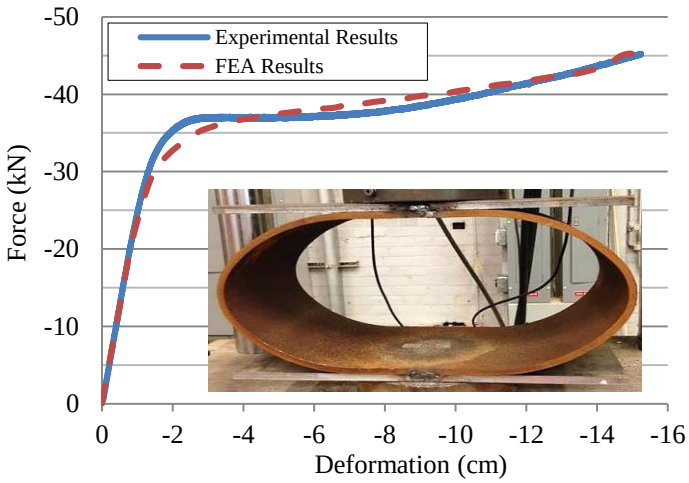

Fig. 12 Force-Deformation Response of a Round HSS16x0.375 and Deformed Configuration at Approximately 152 mm

The sections that were tested are the same sections that were simulated with the boundary plane support/loading condition analysis with material grades noted in Table 2. Sections with different material grades were used in the experiments simply due to local availability. Regardless of the different material grades, the overall intent of these experiments was to provide a proof of concept which is described in the following section. Each round HSS was welded to two 13 mm thick A36 steel plates to simulate the boundary condition analyzed in the FEA described above.

6.2.1. Experimental Testing Results

The results of the experimental testing are displayed along with force-deformation responses in Fig. 10 to Fig. 12. The experimental tests compared well with the results of FEA. Although the results are only presented to a reasonable deformation for building panel connections (152 mm), the tubes were compressed during testing until the inner diameter was near contact (see Fig. 10) while maintaining or increasing its load carrying capacity illustrating the extremely ductile response of the tubes. The HSS7x0.25 section eventually experienced cracking in the outer fibers at approximately 150 mm deformation. Both the experimental and FEA results show that a round HSS is able to provide very desirable force and deformation behavior for BRDC application considered. The experimental results also revealed that only the roundHSS7 experienced cracking at the outer fibers (at approximately 150 mm of deformation and 57° of rotation), but still sustained the load carrying capacity after fracturing until the test was stopped when the inner diameter was in-contact with itself.

7. Conclusions

This study evaluated the feasibility of simple and effective blast resistant ductile connections (BRDC) between the building envelope and primary lateral force resisting system. The structural blast mitigation approach enhances the building envelope ductility and BRDCs act as sacrificial and replaceable elements. A basic theoretical model was developed to predict BRDC and panel response by applying principles of conservation of energy, conservation of momentum, and a generalized single degree of freedom dynamics model. Transient nonlinear finite element analyses were used to verify the theoretical results for BRDC behavior assumed to be elasto-plastic. A practical BRDC design was presented and its energy absorbing capabilities were evaluated through nonlinear finite element analyses and quasi-static experimental testing.

The theoretical evaluation found that for a wide range of blast scenarios a BRDC system was able to fully dissipate the energy from the blast event without damaging the building envelope by plastically yielding through a prescribed displacement. Additionally, it helped to define a practical design range of the panel edge yield force to be greater than 13.3 kN and less than 46.7 kN however increasing panel reinforcement or possibly installing carbon fiber reinforcement on the inside of the panel to provide strength beyond the temperature and shrinkage minimum could further increase resistance by allowing larger BRDC yield forces. Inclusion of BRDC into the system has the potential to significantly increase the blast resistance of the building envelope while possibly preventing damage to the envelope itself. The nonlinear transient FEA of the BRDC-envelope system correlated well with the theoretical results for a range of practical design scenarios. A simple, effective BRDC design that uses standard structural shapes (round HSS) with limited fabrication was proposed and shown through nonlinear static FEA and experimental testing to provide the required force and deformation behavior. The quasi-static experimental testing correlated well with the FEA and verified that a round HSS is able to resist the applied load through the large deformations and strains imposed on the section during loading. A round HSS BRDC is believed to be cost-efficient and provide the necessary performance for the mitigation of blast pressures on building envelope panels.

Further research should investigate building envelope systems that includes panels of various materials and could provide a theoretical formulation with more refined BRDC behavior (however results presented here show that even elasto-plastic behavior gives reasonable results). It may be possible to provide a connector detail capable of resisting both gravity loads of the panel and blast induced pressures. Finally, experimental testing of complete BRDC and envelope panel under quasi-static and dynamic blast pressures is desirable.

8. References

American Concrete Institution (2008). "318-08: Building Code Requirements for Structural Concrete and Commentary." American Concrete Institution, Farmington Hills, MI.

AISC (2005). "Steel Construction Manual Thirteenth Edition." American Institute of Steel Construction, Chicago, IL.

AISC (2010). Seismic Provisions for Structural Steel Buildings. ANSI/AISC 341-10. American Institute of Steel Construction. Chicago, IL.

ASCE (2010). Minimum Design Loads for Buildings and Other Structures. ASCE 7-10. American Society of Civil Engineers. Reston, VA.

ANSYS® Academic Research, Release 14.0, Help System, Mechanical Application User's Guide, ANSYS, Inc.

Biggs, J. M. (1964). *Introduction to Structural Dynamics*. McGraw Hill, New York, NY.

Blevins, R. D. (1993). "Formulas for Natural Frequency and Mode Shape." Krieger Publishing Company, Malabar, FL.

Chapman, L. D., LaHoud, P., Heimdahl, O. (2004). "Safety Assessment for Explosives Risk (SAFER)." Sandia National Laboratories, Albuquerque, NM.

Clough, R.W. and Penzien, J. (1975). *Dynamics of Structures*, McGraw-Hill, Inc., New York, NY.

Dawson, H. and Smilowitz, R. (2005). "Inelastic Dynamic Response of Curtainwall Systems to Blast Loading." ASCE Structures Congress 2005, New York, NY.

Department of Defense (2008). "UFC 3-340-02 Structures to Resist the Effects of Accidental Explosions." Department of Defense, Washington, D.C.

DeRuntz J.A. and Hodge P.G. (1963). "Crushing of a Tube between Rigid Plates." Journal of Applied Mechanics, 30, 391-395

Federal Emergency Management Agency (2005). "Risk Assessment: A How-To Guide to Mitigate Potential Terrorist Attacks against Buildings." Federal Emergency Management Agency, Washington, DC.

Kingery, C. N. (1966). "Air Blast Parameters versus Distance for Hemispherical TNT Surface Bursts." Report BRLR 1344, U. S. Army Material Command Ballistic Research Laboratories, Aberdeen Proving Grounds, MD.

Lavarnway, D. (2013). "Evaluating the Use of Ductile Envelope Connectors for Improved Blast Protection of Buildings." M.S. Thesis. Case Western Reserve University, Cleveland, OH.

Malvar, L., Crawford, J., and Morrill, K. (2007). "Use of Composites to Resist Blast." Journal of Composites for Construction, ASCE, Vol. 11, No. 6, pp. 601 – 610.

Marchand, K. A. and Alfawakhiri, F. (2004). "Facts for Steel Buildings number 2: Blast and Progressive Collapse." American Institute of Steel Construction, Chicago, IL.

Naito, C., Dinan, R., and Bewick, B. (2011). "Use of Precast Concrete Walls for Blast Protection of Steel Stud Construction." Journal of Performance of Constructed Facilities, ASCE, Vol. 25, No. 5, pp. 454-463.

Naito, C. J. and Wheaton, K. P. (2006). "Blast Assessment of Load-Bearing Reinforced Concrete Shear Walls." Practice Periodical on Structural Design and Construction, ASCE, Vol. 11, No. 2, pp. 112-121.

Okazaki, T. (2004). "Seismic Performance of Link-to-Column Connections in Steel Eccentrically Braced Frames." Ph.D. Dissertation. University of Texas, Austin, TX.

Parker, James (2008). "Facade Attachments to Steel-Framed Buildings." American Institute of Steel Construction, Chicago, IL.

Redwood, R. (1964). "Discussion of Crushing of a Tube between Rigid Plates (DeRuntz and Hodge, 1963)." Journal of Applied Mechanics, 31, 357-358.

Reid, S. and Reddy, T. (1977). "Effects of Strain Hardening on the Lateral Compression of Tubes between Rigid Plates." International Journal of Solid Structures, 14, 213-225.

Seica, M., Krynski, M., Walker, M., and Packer, J. (2011). "Analysis of Dynamic Response of Architectural Glazing Subjected to Blast Loading." Journal of Architectural Engineering, ASCE, Vol. 17, No. 2, pp. 59 – 74.

Silva, P. and Lu, B. (2009). "Blast Resistance Capacity of Reinforced Concrete Slabs." Journal of Structural Engineering, ASCE, Vol. 135, No. 6, pp. 708-716.

Swisdak, M. M. (1994). "Simplified Kingery Airblast Calculations." Naval Surface Warfare Center, Indian Head Division, Silver Spring, MD.

Urgessa, G. and Maji, A. (2010). "Dynamic Response of Retrofitted Masonry Walls for Blast Loading." Journal of Engineering Mechanics, ASCE, Vol. 136, No. 7, pp. 858-864.

Weggel, D. and Zapata, B. (2008). "Laminated Glass Curtain Walls and Laminated Glass Lites Subjected to Low-Level Blast Loading." Journal of Structural Engineering, ASCE, Vol. 134, No. 3, pp. 466-477.